

Igor Poljak

E-mail: ipoljak1@unizd.hr

Jelena Čulin

E-mail: jculin@unizd.hr

Department of Maritime Sciences, University of Zadar, Mihovila Pavlinovića 1,
23000 Zadar, Croatia

Vedran Mrzljak

E-mail: vedran.mrzljak@riteh.uniri.hr

Faculty of Engineering, University of Rijeka, Vukovarska 58, 51000 Rijeka, Croatia

Vlatko Knežević

E-mail: vknezevil@unizd.hr

Department of Maritime Sciences, University of Zadar, Mihovila Pavlinovića 1,
23000 Zadar, Croatia

LNG Carrier Steam Dump Process Analysis

Abstract

At the conventional LNG (Liquefied Natural Gas) carrier during the port operation, maintaining cargo tank pressure can be a challenging task. This task can be obtained through steam dump only, if the superheated steam line is not in operation. This paper presents an analysis of a steam dump process from a conventional LNG carrier. It is shown that steam dump process produces around 8 times lower harmful environmental emissions than releasing pure methane in the atmosphere. Simultaneously, steam produced by gas combustion must be mixed with feed water to ensure its dry saturation – only saturated steam can condense in the main condenser. The paper shows feed water mass flow rate calculation procedure at various desuperheated steam mass flow rates and temperatures to ensure proper dry saturation process. Also, the exergy destruction and exergy efficiency of the feed water and desuperheated steam mixing process are calculated, presented and discussed.

Keywords: Steam dump, Global warming potential, Conventional LNG carrier, Energy balancing, Exergy analysis

1. Introduction

A large number of conventional LNG (Liquefied Natural Gas) carriers use the steam power plant [1-3]. This technology is mature, many times proven reliable and its maintenance costs less compared to the other power plant solutions [4, 5]. However, the steam power plant has lower efficiency in comparison to other propulsion solutions on the market, and therefore it is not any more option for the propulsion power of modern LNG carriers [6, 7]. Q-Flex and Q-Max LNG carriers consume the same amount of HFO (Heavy Fuel Oil) as conventional LNG carriers, but they carry more cargo. Since they use nitrogen as a refrigerant for the liquefaction of the evaporated cargo and they do not use gas consumption for the propulsion machinery, they are also an obsolete concept. The reason is the fact that the burning of HFO produces large amounts of air pollutants [8]. The last LNG carriers' generation uses a combination of HFO and gas, and gas only and therefore emits lower pollutant quantities. Also, they use less fuel due to an increase in internal combustion engine efficiency [9, 10]. Therefore, they must have better cargo tank insulation, which allows a lower boil-off rate. Compared to conventional LNG carriers, where the boil-off rate was 0.125 % per day, the boil-off rate on modern LNG carriers is 0.085 % of the cargo per day only [11].

From the first to the last generation of LNG carriers, various techniques were used to maintain the cargo tank pressure while transporting cargo from the loading to the discharging port [12, 13]. Since the typical lifespan of an LNG carrier is around 30 to 35 years, conventional LNG carriers are still in service. Therefore, this article will present how the cargo temperature and pressure are maintained on the conventional LNG carrier and what methods are in disposition when the vessel is underway, anchored, or alongside the port.

2. Methods for maintaining cargo temperature and pressure

The conventional steam LNG carriers are equipped with two symmetrical steam generators, which have the following burning modes: diesel oil burning mode, heavy fuel oil burning mode, gas burning mode and dual burning mode, i.e. heavy fuel oil and natural gas mode at the same time and under various mixing ranges [14]. Under sea-going conditions, conventional LNG carriers maintain the tank pressure by burning the excess evaporated gas in the boilers.

The concept of maintaining the cargo tank pressure is shown in Table 1. It may be seen that operating points 1 and 2 are not allowed areas of operation due to low pressure in the tank, close to the atmospheric pressure. If the tank pressure decreases below atmospheric pressure, then the cargo tank may collapse. The protection method is first to secure all boil-off gas supply from the cargo tank to the machinery, and if that doesn't help then opening the cargo tank safety valve prevents the creation of a vacuum inside the cargo tank. Therefore, the minimum tank pressure is 0.102 MPa.

Operating points from 3 to 25 represents allowable tank pressure variations. From Table 1 it can be seen that increase in tank pressure simultaneously increases cargo temperature and decreases cargo density as well as gross heating value.

In operating point 26 the safety valve opens again to protect the cargo tank and the ship structure from overpressure in the cargo tank and that area should not be reached. Normally, cargo in the port is loaded between operating points from 8 to 11 at the pressure from 0.107 to 0.110 MPa. While the vessel is underway, if tank pressure is maintained below loading pressure, then the cargo temperature decreases. On the other side, if the cargo pressure increases above the loading pressure then the temperature of the cargo will increase too (Table 1) [15]. Maintaining cargo tank pressure at loading value on the conventional LNG carriers can be done by varying load on the main boilers, which is easy to achieve if the vessel is underway by increasing or decreasing speed. This is a reason why this type of LNG carrier continues to sail until the last moment before the pilot arrives.

Table 1. Expected pressure rise for the loaded cargo (LNG) - from operating point 1 (0.100 MPa) up to operating point 26 (0.125 MPa).

Operating point	Temperature (°C)	Pressure (MPa)	Density (kg/m ³)	Specific enthalpy (kJ/kg)	Specific entropy (kJ/kg-K)	Gross Heating value (Liquid) (kJ/kg)
1	-161.96	0.100	459.77	-28.385	-0.004573	55861
2	-161.83	0.101	459.60	-27.980	-0.000955	55857
3	-161.70	0.102	459.42	-27.579	0.002632	55853
4	-161.58	0.103	459.25	-27.180	0.006188	55849
5	-161.45	0.104	459.08	-26.784	0.009714	55845
6	-161.33	0.105	458.91	-26.391	0.013210	55842
7	-161.21	0.106	458.74	-26.001	0.016678	55838
8	-161.09	0.107	458.57	-25.614	0.020116	55834
9	-160.97	0.108	458.40	-25.229	0.023527	55830
10	-160.85	0.109	458.24	-24.847	0.026910	55827
11	-160.73	0.110	458.07	-24.468	0.030266	55823
12	-160.61	0.111	457.91	-24.091	0.033596	55819
13	-160.49	0.112	457.74	-23.717	0.036899	55816
14	-160.37	0.113	457.58	-23.346	0.040177	55812
15	-160.26	0.114	457.42	-22.977	0.043429	55809
16	-160.14	0.115	457.26	-22.610	0.046656	55805
17	-160.03	0.116	457.10	-22.246	0.049860	55802

18	-159.92	0.117	456.94	-21.884	0.053039	55799
19	-159.80	0.118	456.79	-21.524	0.056194	55795
20	-159.69	0.119	456.63	-21.116	0.059326	55792
21	-159.58	0.120	456.48	-20.811	0.062435	55789
22	-159.47	0.121	456.32	-20.458	0.065522	55785
23	-159.36	0.122	456.17	-20.108	0.068587	55782
24	-159.25	0.123	456.02	-19.759	0.071629	55779
25	-159.14	0.124	455.86	-19.413	0.074650	55776
26	-159.03	0.125	455.71	-19.068	0.077650	55773

At the port and at the anchor the main propulsion system is not running, so the steam demand of the main boilers is reduced. In that case, tank pressure is raised above the values requested by the receiving terminals (0.107 to 0.112 MPa). That request is due to several terminal variables. The low pressure value is important due to the limited capacity and the power of the boil-off gas return compressor and the length of the return line. Also, if there is no adequate gas consumption in the terminal storage tank then the pressure in the storage tank will increase and consequently, gas must be burned, which is not desirable for the buyer.

Therefore, if the load is increased and the ship is in the port or at anchor, there will be an excess of the energy that must be dumped. If the boil-off gas exceeds the requirements for normal steam production, steam production is increasing further to maintain the cargo tank pressure in the balance by burning excess boil-off gas from the cargo tank. That surplus of the produced steam in the steam generators is then dumped into the steam production system again or released into the air. The steam dump concept is designed to prevent the cargo tank safety valve opening at tank pressure of 25 kPa above atmospheric pressure. If the cargo tank safety valve opens, then the cargo vapors will be released from the cargo tank into the atmosphere. The main component of natural gas by the molar fraction is methane, the greenhouse gas, and its release is not allowed except in emergencies according to The International Convention for the Prevention of Pollution from Ships (MARPOL 73/78), Annex VI [16]. To avoid such scenario, burning the gas is compulsory. Emitting carbon dioxide and other combustion products is more environmentally friendly than emitting methane. Namely, the Global Warming Potential (GWP) of methane is about 28, much higher than carbon dioxide, whose GWP is 1 [17, 18]. Taking into account the problem of global warming, concept of excess boil-off gas burning in the main boilers is a useful one despite the wasted energy.

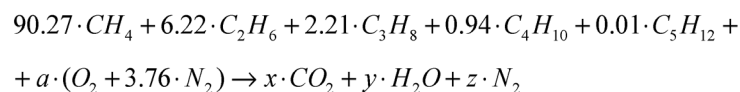
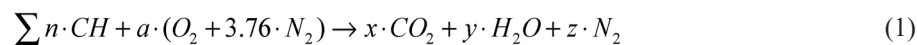
The benefit of the vaporized cargo combustion process in comparison to releasing pure methane in the air can be illustrated by the following example.

The typical composition of the natural gas for the three various loading ports is given in Table 2 [19]. For illustration purposes, the composition of the natural gas from the loading port in Qatar, Ras Laffan is chosen.

Table 2. The molar fraction of natural gas in three various ports.

Molar fraction	Ras Laffan	Das Islands	Darwin
CH ₄	0.9027	0.8654	0.8784
C ₂ H ₆	0.0622	0.1150	0.0937
C ₃ H ₈	0.0221	0.0152	0.0225
n-C ₄ H ₁₀	0.0056	0	0.0018
i- C ₄ H ₁₀	0.0038	0	0.0020
n-C ₅ H ₁₀	0.0001	0	0.0003
N ₂	0.0035	0.0044	0.0013
Σ	1.0000	1.0000	1.0000

The stoichiometry relation of the chosen cargo combustion is [20]:



where:

$$C \rightarrow b = x$$

$$H \rightarrow 2 \cdot c = y$$

$$O_2 \rightarrow a = b + \frac{c}{2}$$

$$N_2 \rightarrow z = a \cdot 3.76 \quad (2)$$

$$C \rightarrow b = x = 113.15 \text{ [mol]}$$

$$H \rightarrow 2 \cdot c = y = 212.8 \text{ [mol]}$$

$$O_2 \rightarrow a = b + \frac{c}{2} = 219.55 \text{ [mol]}$$

$$N_2 \rightarrow z = a \cdot 3.76 = 825.508 \text{ [mol]}$$

$$90.27 \cdot CH_4 + 6.22 \cdot C_2H_6 + 2.21 \cdot C_3H_8 + 0.94 \cdot C_4H_{10} + 0,01 \cdot C_5H_{12} + 219.55 \cdot \\ \cdot (O_2 + 3.76 \cdot N_2) \rightarrow 113.15 \cdot CO_2 + 212.8 \cdot H_2O + 825.508 \cdot N_2$$

In the equations above CO_2 is carbon dioxide, H_2O is water vapor, N_2 is nitrogen and O_2 is oxygen.

The mole fractions of the product gases are determined as follows:

$$n_{prod} = \sum (CO_2 + H_2O + N_2) \quad (3)$$

$$n_{prod} = 113.15 + 212.8 + 825.508 = 1151.458 \text{ [mol]}$$

$$\phi = \frac{n_\phi}{n_{prod}} \quad (4)$$

$$\phi_{CO_2} = \frac{n_{CO_2}}{n_{prod}} = \frac{113.15}{1151.458} = 0.0983 = 9.83 \%$$

$$\phi_{H_2O} = \frac{n_{H_2O}}{n_{prod}} = \frac{212.8}{1151.458} = 0.1848 = 18.48 \%$$

$$\phi_{N_2} = \frac{n_{N_2}}{n_{prod}} = \frac{825.508}{1151.458} = 0,7169 = 71.69 \%$$

The combustion of 100 mol of fuel gives 113.15 mol of carbon dioxide and 212.8 mol of water vapor as the combustion products. The GWP (Global Warming Potential) of the water vapor is in the range from -0.001 to 0.0005 and it does not alter the climate [21, 22]. Taking into account GWP, the quantity of produced CO_2 (4978.6 kg) corresponds to 177.8 kg of CH_4 . Releasing cargo vapors directly into the atmosphere brings 90.27 mol (1444.32 kg) of CH_4 (8.12 times higher amount). It should

be highlighted that considering natural gas composition from any other port presented in Table 2 will give different mole fraction values of the product gases, but the main conclusions related to the GWP presented above will remain the same regardless of the selected natural gas composition.

3. Steam dump process on the LNG carrier Grace Barleria

Excess boil-off gas burning in the steam generators reduces GWP (as proven in a previous paper Section), but it simultaneously produces a notable superheated steam mass flow rate, which cannot be completely used in steam power plant system. Therefore, the excess steam mass flow rate must be released from the power plant and sent to the main condenser through dump line. Steam dump line must be able to prepare excess steam mass flow rate (desuperheated steam, Figure 1) in a way that steam reaches the saturation state. Only the saturated steam is able to condense in main condenser.

The model for the description of the desuperheated steam balancing process (to reach dry saturation state) is taken from ship Grace Barleria, which is a conventional LNG carrier. The main particulars of the vessel can be found in [14, 23]. The dump system takes the steam from the main boiler, desuperheating line. Desuperheated steam is taken from the superheated steam line, but passes again through the steam drum where the pressure remains the same, but the temperature decreases, from around 525 °C to about 300 - 400 °C. After passing the steam drum, desuperheated steam goes to the pressure reducing station [24], where the pressure is lowered from the main boiler pressure of 6 MPa to main condenser pressure. The feed water injected in desuperheated steam cools it [25] to reach saturation temperature (dry saturation state) before entering the main condenser. The dump line after the pressure-reducing valve is divided into two parallel lines, each of capacity 50 % of the total steam dump. The temperature of the main condenser should be less than 70 °C and the pressure should be below 0.021 MPa. Otherwise, main turbine cannot run in its designed area, but is tripping to protect internal parts [26]. The amount of feed water which has to be filled in the dump line along with the desuperheated steam will be determined later in the paper. Figure 1 shows the desuperheating line and dump overview layup.

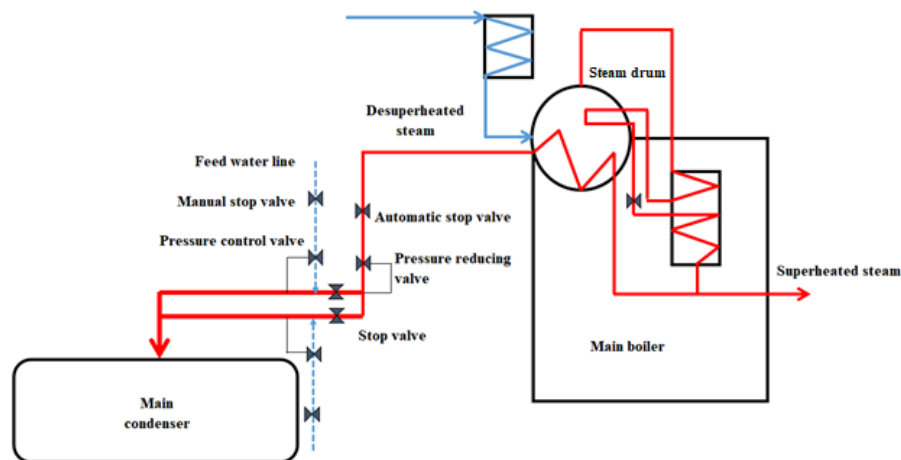


Figure 1. Desuperheating line and dump overview layout.

4. Energy balancing of the steam dump line

The energy balancing principle is well known from the literature [27]. The energy balance principle related to any observed system, plant or a component is based on equalizing cumulative energy inlet into the observed volume and cumulative energy outlet from the observed volume.

Accordingly, it follows that entering streams are feed water and desuperheated steam. The exiting stream is dry saturated steam, Figure 2.

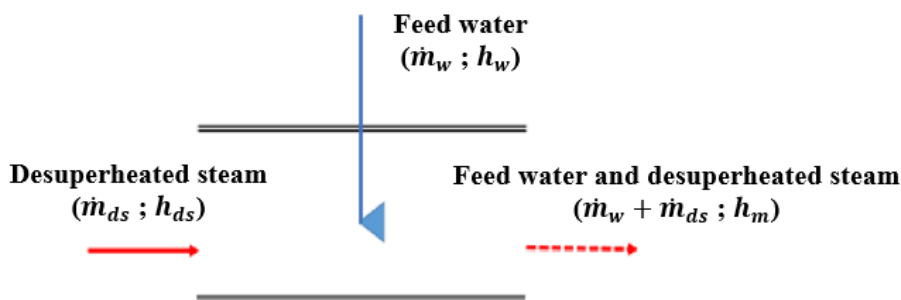


Figure 2. Mass balancing of desuperheating line.

Energy balance equation is:

$$\dot{m}_{ds} \cdot h_{ds} + \dot{m}_w \cdot h_w = \dot{m}_w \cdot h_m + \dot{m}_{ds} \cdot h_m \quad (5)$$

where are:

\dot{m}_w - feed water mass flow rate [kg/s]

\dot{m}_{ds} - desuperheated steam mass flow rate [kg/s]

h_w - feed water specific enthalpy [kJ/kg]

h_{ds} - desuperheated steam specific enthalpy [kJ/kg]

h_m - specific enthalpy of dry saturated steam [kJ/kg]

Required feed water mass flow rate for the desuperheated steam transferring to a dry saturated state is derived from Equation 5:

$$\dot{m}_{ds} \cdot h_{ds} + \dot{m}_w \cdot h_w = \dot{m}_w \cdot h_m + \dot{m}_{ds} \cdot h_m$$

$$\dot{m}_w \cdot h_w - \dot{m}_w \cdot h_m = \dot{m}_{ds} \cdot h_m - \dot{m}_{ds} \cdot h_{ds}$$

$$\dot{m}_w = \frac{\dot{m}_{ds} \cdot (h_m - h_{ds})}{(h_w - h_m)} \quad (6)$$

The required feed water mass flow rate which has to be sprayed in desuperheated steam depends on the pressure in the main condenser, sea temperature, desuperheated steam mass flow rate as well as on the feed water and desuperheated steam pressure and temperature.

In cold sea conditions, main condenser pressure remains constant, so the specific enthalpy of dry saturated steam (h_m in Equation 6) also remains constant. By knowing feed water and desuperheated steam pressure and temperature (and therefore specific enthalpies h_w and h_{ds} in Equation 6) at the specific main condenser pressure, mass flow rate of water which has to be sprayed in the dump line for desuperheated steam dry saturation depends on the desuperheated steam mass flow rate only.

In Table 3 is presented feed water mass flow rate required for the dry saturation of desuperheated steam at the main condenser constant pressure equal to 0.0044 MPa.

Table 3 is presented for various desuperheated steam mass flow rates. Desuperheated steam pressure and temperature before pressure reducing valve, Figure 1, were 300 °C and 6 MPa (corresponding specific enthalpy is 2885.5 kJ/kg). Pressure reducing valve reduces desuperheating steam pressure to the main condenser pressure,

while specific enthalpy remains unchanged. Therefore, at the entrance of mixing point, Figure 2, desuperheated steam pressure is equal to one in the main condenser, while specific enthalpy is $h_{ds} = 2885.5$ kJ/kg. Feed water in mixing point has pressure equal to one in the main condenser, while its specific enthalpy is $h_w = 128.32$ kJ/kg. After the mixing, dry saturated steam has specific enthalpy $h_m = 2556.7$ kJ/kg and pressure equal to one in the main condenser. Specific enthalpies of feed water, desuperheated steam and dry saturated steam remains the same for all desuperheated steam mass flow rates presented in Table 3. Specific enthalpies of all flow streams are calculated by using NIST-Refprop 9.0 software [15].

Table 3. Mass flow rate of feed water required for the desuperheated steam dry saturation at the main condenser constant pressure 0.0044 MPa

Desuperheated steam mass flow rate - \dot{m}_{ds} [kg/h]	Feed water mass flow rate - \dot{m}_w [kg/h]
1000	135.40
2000	270.80
3000	406.20
4000	541.60
5000	676.99
6000	812.39
7000	947.79
8000	1083.19
9000	1218.59
10000	1353.99

Desuperheated steam temperature before pressure reducing valve can vary. The feed water mass flow rates required for the desuperheated steam dry saturation at various desuperheated steam temperatures at the pressure reducing valve inlet are presented in Table 4.

In Table 4, desuperheated steam temperature before pressure reducing valve is varied between 300 °C and 390 °C, while the pressure of that steam is 6 MPa for all temperatures. After pressure reducing valve, desuperheated steam specific enthalpy (h_{ds}) remains the same as before pressure reducing valve, for each temperature. Desuperheated steam mass flow rate is equal to 10000 kg/h, while main condenser pressure is 0.0044 MPa for each desuperheated steam temperature. Feed water in mixing point has pressure equal to one in the main condenser and specific enthalpy $h_w = 128.32$ kJ/kg for each desuperheated steam temperature. After the mixing, dry saturated steam has pressure equal to the main condenser pressure and specific enthalpy $h_m = 2556.7$ kJ/

kg for each desuperheated steam temperature. Specific enthalpies of all flow streams are calculated by using NIST-Refprop 9.0 software [15]. From the corresponding specific enthalpies are calculated required feed water mass flow rates using Equation 6, for the desuperheated steam dry saturation.

Table 4. Feed water mass flow rates required for the desuperheated steam dry saturation at various desuperheated steam temperatures before pressure reducing valve

Desuperheated steam temperature before pressure reducing valve - t_{ds} [°C]	Desuperheated steam specific enthalpy before and after pressure reducing valve - h_{ds} [kJ/kg]	Feed water mass flow rate - \dot{m}_w [kg/h]
300	2885.5	1353.99
310	2920.6	1498.53
320	2953.6	1634.42
330	2984.9	1763.32
340	3014.9	1886.85
350	3043.9	2006.28
360	3072.0	2121.99
370	3099.4	2234.82
380	3126.1	2344.77
390	3152.4	2453.08

The main conclusions which can be derived from Table 3 and Table 4 are that an increase in desuperheated steam mass flow rate as well as an increase in desuperheated steam temperature before pressure reducing valve will simultaneously require more and more feed water for the steam dry saturation process.

The efficiency and losses of the feed water and desuperheating steam mixing process (with an aim to obtain dry saturated steam) cannot be calculated from the energy viewpoint, because energy balance, Equation 5, is used for the required feed water mass flow rate calculation. Therefore, the efficiency and losses of the mentioned process are calculated by using exergy approach.

In comparison to energy analysis of any system or process, which did not consider parameters of the ambient in which the system or process operates, exergy analysis considers these parameters [28-30]. In the literature can be found many examples of the exergy analysis application in marine sector [31-33]. For each exergy analysis is required to define the base ambient state [34, 35]. In this analysis, the base ambient state is defined by the ambient temperature of 25 °C and the ambient pressure of 0.1 MPa.

For the observed desuperheated steam and feed water mixing process, exergy destruction (exergy losses) can be calculated by an equation [36]:

$$\dot{E}x_D = \dot{m}_{ds} \cdot \varepsilon_{ds} + \dot{m}_w \cdot \varepsilon_w - \left(\dot{m}_w + \dot{m}_{ds} \right) \cdot \varepsilon_m \quad (7)$$

where is specific exergy of each observed fluid stream, which definition can be found in the literature [37, 38]. Exergy efficiency of desuperheated steam and feed water mixing process is:

$$\eta_{ex} = \frac{(\dot{m}_w + \dot{m}_{ds}) \cdot \varepsilon_m}{\dot{m}_{ds} \cdot \varepsilon_{ds} + \dot{m}_w \cdot \varepsilon_w} \quad (8)$$

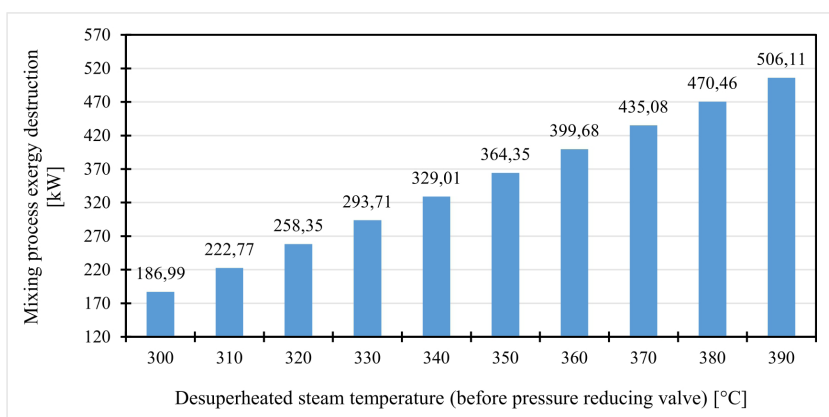


Figure 3. Mixing process exergy destruction in relation to desuperheated steam temperature

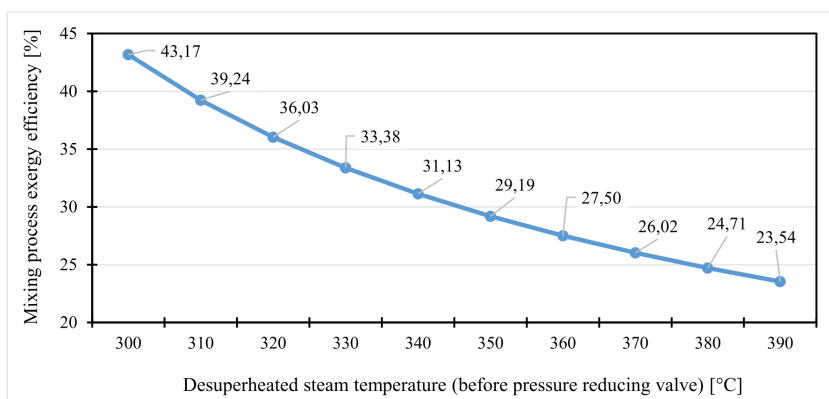


Figure 4. Mixing process exergy efficiency in relation to desuperheated steam temperature

Figure 3 and Figure 4 reveals that an increase in desuperheated steam temperature before pressure reducing valve simultaneously increases mixing process exergy destruction and decreases the same mixing process exergy efficiency. At the lowest observed desuperheated steam temperature before pressure reducing valve of 300 °C mixing process exergy destruction is equal to 186.99 MW, while at the highest observed desuperheated steam temperature before pressure reducing valve of 390 °C mixing process exergy destruction is equal to 506.11 MW (at the same desuperheated steam temperature of 390 °C mixing process exergy efficiency is equal to 23.54 % only). Even at low desuperheating steam temperatures, mixing process exergy efficiency is very low (it did not reach 45 %) – such low exergy efficiency confirms that the main goal of this mixing process is not to be optimal in any way, the main goal is to ensure steam condensation and releasing excess energy from the steam system.

5. Conclusion

Maintaining cargo pressure is an important requirement imposed by buyers. At the conventional LNG carrier in the port, it can be done by the steam dump process only, if the superheated steam line is not in operation.

Steam dump process represents a waste of energy, but it is a useful concept in the marine and shore industry due to the lower global warming potential in comparison to CH₄, which is the main component of LNG. As shown in the presented example, the quantity of emitted CO₂ can be around 8 times less harmful to the atmosphere than the corresponding quantity of released CH₄, if the excess boil-off gas combustion is applied.

Unfortunately, there is still no technical solution which will use the released energy from the cargo tank while the ship is not underway. The storage of the electrical energy in the batteries may help in that respect. The stored energy could be the source of the power supply for the accommodation or the propulsion. Such a solution may increase the total efficiency of the ship steam power plant.

Acknowledgments

The research has been supported by the Croatian Science Foundation under the project IP-2022-10-2821.

Literature

1. Fernández, I. A., Gómez, M. R., Gómez, J. R., & Insua, Á. B. (2017). Review of propulsion systems on LNG carriers. *Renewable and Sustainable Energy Reviews*, 67, 1395-1411. (doi:10.1016/j.rser.2016.09.095)
2. Poljak, I., & Mrzljak, V. (2023). Thermodynamic Analysis and Comparison of Two Marine Steam Propulsion Turbines. *NAŠE MORE: znanstveni časopis za more i pomorstvo*, 70(2), 0-0. (doi:10.17818/NM/2023/2.2)

3. Huan, T., Hongjun, F., Wei, L., & Guoqiang, Z. (2019). Options and evaluations on propulsion systems of LNG carriers. *Propulsion systems*, 1.
4. Hiramatsu, S., Hiraoka, K., Fujino Y., Tsumura, K. (2010) Technology Trends and MHI Activities for LNG Carriers-Diverse Shipbuilding and Marine Products in the LNG Supply Chain. *Mitsubishi Heavy Industries Technical Review* 47 (3).
5. Poljak I., Orović J., Knežević V., Mrzljak V. (2020) LNG Carrier Main Steam Turbine Reliability in the Exploitation Period of Time. *TransNav, the International Journal on Marine Navigation and Safety of Sea Transportation*. 14 (1) 39-42. (doi:10.12716/1001.14.01.03)
6. Zhu, L., Li, B., Li, A., Ji, W., Qian, Y., Lu, X., & Huang, Z. (2020). Effects of fuel reforming on large-bore low-speed two-stroke dual fuel marine engine combined with EGR and injection strategy. *International Journal of Hydrogen Energy*, 45(53), 29505-29517. (doi:10.1016/j.ijhydene.2020.07.266)
7. Coraddu, A., Oneto, L., Ilardi, D., Stoumpos, S., & Theotokatos, G. (2021). Marine dual fuel engines monitoring in the wild through weakly supervised data analytics. *Engineering Applications of Artificial Intelligence*, 100, 104179. (doi:10.1016/j.engappai.2021.104179)
8. Mrzljak, V., Poljak, I., Kosor, M., Čulin, J. (2023) Bisection Method for the Heavy Fuel Oil Tank Filling Problem at a Liquefied Natural Gas Carrier. *Journal of Marine Science and Engineering*. 11, 849. (doi:10.3390/jmse11040849)
9. Theotokatos, G., Stoumpos, S., Bolbot, V., & Boulougouris, E. (2020). Simulation-based investigation of a marine dual-fuel engine. *Journal of Marine Engineering & Technology*, 19(sup1), 5-16. (doi:10.1080/20464177.2020.1717266)
10. Yu, H., Wang, W., Sheng, D., Li, H., & Duan, S. (2022). Performance of combustion process on marine low speed two-stroke dual fuel engine at different fuel conditions: Full diesel/diesel ignited natural gas. *Fuel*, 310, 122370. (doi:10.1016/j.fuel.2021.122370)
11. Colson, D. Inside The GTT newsletter - March 2021 - n° 20, chrome-extension://efaidnbmnnnibpcajpcjgclcfefindmkaj/https://gtt.fr/sites/default/files/gtt_inside_ndeg20_mars2021_0.pdf, (Accessed: 01/05/2024)
12. Wang, C., Ju, Y., & Fu, Y. (2021). Dynamic modeling and analysis of LNG fuel tank pressurization under marine conditions. *Energy*, 232, 121029. (doi:10.1016/j.energy.2021.121029)
13. Jo, Y., Shin, K., & Hwang, S. (2021). Development of dynamic simulation model of LNG tank and its operational strategy. *Energy*, 223, 120060. (doi:10.1016/j.energy.2021.120060)
14. Mrzljak, V., Poljak, I., & Medica-Viola, V. (2017). Dual fuel consumption and efficiency of marine steam generators for the propulsion of LNG carrier. *Applied thermal engineering*, 119, 331-346. (doi:10.1016/j.applthermaleng.2017.03.078)
15. Lemmon, E. W., Huber, M. L., & McLinden, M. O. (2010). NIST Standard Reference Database 23, Reference Fluid Thermodynamic and Transport Properties (REFPROP), version 9.0, National Institute of Standards and Technology. R1234yf. fld file dated December, 22, 2010.
16. Stephenson, P., Singleton, R., Wagner, C. What pollution legislation is specific to LNG / LPG Cargo? *Standard Bulletin*, March 2011. chrome-extension://efaidnbmnnnibpcajpcjgclcfefindmkaj/https://www.standard-club.com/fileadmin/uploads/standardclub/Documents/Import/publications/bulletins/split-articles/2011/1558044-what-pollution-legislation-is-specific-to-lng-lpg-cargo.pdf (Accessed: 01/05/2024)
17. Mar, K.A., Unger, C., Walderdorff, L., Butler, T. (2022) Beyond CO2 equivalence: The impacts of methane on climate, ecosystems, and health, *Environmental Science & Policy*. 134, pp 127-136. (doi:10.1016/j.envsci.2022.03.027)
18. Balcombe, P., Speirs, J. F., Brandon, N. P., & Hawkes, A. D. (2018). Methane emissions: choosing the right climate metric and time horizon. *Environmental Science: Processes & Impacts*, 20(10), 1323-1339. (doi:10.1039/C8EM00414E)
19. Natural Gas Mining Association, Natural Gas Material 1972-6, Cargo Manual, Mitsubishi Shipbuilding.
20. Cengel, Y. A., Boles, M. A., & Kanoğlu, M. (2011). *Thermodynamics: an engineering approach* (Vol. 5, p. 445). New York: McGraw-hill.
21. Sherwood, S.C.; Dixit, V., Salomez, C. (2018). The global warming potential of near-surface emitted water vapour. *Environmental Research Letters*. 13(10) 104006, (doi:10.1088/1748-9326/aee018)

22. Sherwood, S. C., Dixit, V. V., & Salomez, C. (2018, December). The radiative forcing and Global Warming Potential of near-surface water vapor emissions. In AGU Fall Meeting Abstracts (Vol. 2018, pp. A21H-2774).
23. Mrzljak, V., Poljak, I., & Mrakovčić, T. (2017). Energy and exergy analysis of the turbo-generators and steam turbine for the main feed water pump drive on LNG carrier. *Energy conversion and management*, 140, 307-323. (doi:10.1016/j.enconman.2017.03.007)
24. Mrzljak, V., Poljak, I., & Žarković, B. (2018). Exergy analysis of steam pressure reduction valve in marine propulsion plant on conventional LNG carrier. *NAŠE MORE: znanstveni časopis za more i pomorstvo*, 65(1), 24-31. (doi:10.17818/NM/2018/1.4)
25. Mrzljak, V., Senčić, T., Poljak, I., & Medica-Viola, V. (2022). Thermodynamic Analysis of Steam Cooling Process in Marine Power Plant by Using Desuperheater. *Pomorski zbornik*, 62(1), 9-30.
26. LNG Grace Barleria, Machinery Operating Manual, Hyundai Heavy Industries.
27. Mrzljak, V., Poljak, I., Jelić, M., & Prpić-Oršić, J. (2023). Thermodynamic Analysis and Improvement Potential of Helium Closed Cycle Gas Turbine Power Plant at Four Loads. *Energies*, 16(15), 5589. (doi:10.3390/en16155589)
28. Kanoğlu, M., Çengel, Y. A., & Dinçer, İ. (2012). Efficiency evaluation of energy systems. Springer Science & Business Media.
29. Mrzljak, V., Jelić, M., Poljak, I., & Prpić-Oršić, J. (2023). Analysis and comparison of main steam turbines from four different thermal power plants. *Pomorstvo*, 37(1), 58-74. (doi:10.31217/p.37.1.6)
30. Elhelw, M., Al Dahma, K. S., & el Hamid Attia, A. (2019). Utilizing exergy analysis in studying the performance of steam power plant at two different operation mode. *Applied Thermal Engineering*, 150, 285-293. (doi:10.1016/j.applthermaleng.2019.01.003)
31. Baressi Šegota, S., Lorencin, I., Anđelić, N., Mrzljak, V., & Car, Z. (2020). Improvement of marine steam turbine conventional exergy analysis by neural network application. *Journal of Marine Science and Engineering*, 8(11), 884. (doi:10.3390/jmse8110884)
32. Koroglu, T., & Sogut, O. S. (2018). Conventional and advanced exergy analyses of a marine steam power plant. *Energy*, 163, 392-403. (doi:10.1016/j.energy.2018.08.119)
33. Baressi Šegota, S., Mrzljak, V., Anđelić, N., Poljak, I., & Car, Z. (2023). Use of Synthetic Data in Maritime Applications for the Problem of Steam Turbine Exergy Analysis. *Journal of marine science and engineering*, 11(8), 1595. (doi:10.3390/jmse11081595)
34. Szargut, J. (2005). Exergy method: technical and ecological applications (Vol. 18). WIT press.
35. Mrzljak, V., Poljak, I., Prpić-Oršić, J., & Jelić, M. (2020). Exergy analysis of marine waste heat recovery CO₂ closed-cycle gas turbine system. *Pomorstvo*, 34(2), 309-322. (doi:10.31217/p.34.2.12)
36. Erdem, H. H., Akkaya, A. V., Cetin, B., Dagdas, A., Sevilgen, S. H., Sahin, B., ... & Atas, S. (2009). Comparative energetic and exergetic performance analyses for coal-fired thermal power plants in Turkey. *International Journal of Thermal Sciences*, 48(11), 2179-2186. (doi:10.1016/j.ijthermalsci.2009.03.007)
37. Uysal, C., Kurt, H., & Kwak, H. Y. (2017). Exergetic and thermoeconomic analyses of a coal-fired power plant. *International Journal of Thermal Sciences*, 117, 106-120. (doi:10.1016/j.ijthermalsci.2017.03.010)
38. Mrzljak, V., Žarković, B., & Poljak, I. (2017). Energy and exergy analysis of sea water pump for the main condenser cooling in the LNG carrier steam propulsion system. *Mathematical Modeling*, 1(3), 144-147.

